

Modern Physics Letters A
 © World Scientific Publishing Company

k_t - factorization and CCFM **the solution for describing the hadronic final states - everywhere ?**

Hannes Jung

*Department of Physics, Lund University, Box 118
 Lund, 22100
 Sweden
 hannes.jung@desy.de*

Received (Day Month Year)

Revised (Day Month Year)

The basic ideas of k_t -factorization and CCFM parton evolution is discussed. The unintegrated gluon densities, obtained from CCFM fits to the proton structure function data at HERA are used to predict hadronic final state cross sections like jet production at HERA, but also comparisons with recent measurements of heavy quark production at the Tevatron are presented. Finally, the k_t -factorization approach is applied to Higgs production at high energy hadron hadron colliders and the transverse momentum spectrum of Higgs production at the LHC is calculated.

This paper is dedicated to the memory of Bo Andersson and Jan Kwiecinski, who inspired so much in the field of small- x physics and passed away too early.

Keywords: Keyword1; keyword2; keyword3.

PACS Nos.: include PACS Nos.

1. Introduction

The theory of strong interaction, QCD, has been very successful in describing many experimental measurements, but a number of problems have not yet been solved, some of which are related to the transition between the perturbative and non-perturbative region. The perturbative methods, however, work surprisingly well, even down to very low scales, where the running coupling constant, α_s , starts to become large. Another type of problem is related to the observation, that at high energies, even for small values of coupling constant α_s , the phase space for parton emissions increases fast, and that therefore it is not sufficient to include only a few calculable terms in the perturbative expansion. This problem can be treated by resumming the leading logarithmic behavior of the cross section. The most important contribution at small x is gluon bremsstrahlung, with the typical behavior of being largest in the infrared and/or collinear region. Two different resummation strategies have been developed: the DGLAP [1,2,3,4] approach, resumming leading logarithms of ratios of subsequent virtualities also called collinear approach, and

2 Hannes Jung

the BFKL [5, 6, 7] approach, resumming the infrared contributions, also called the k_t -factorization [8, 9] or the semi-hard approach [10, 11]. The CCFM [12, 13, 14, 15] approach attempts to cover both the collinear and the infrared regions by considering color coherence effects, and in the limit of asymptotic energies is almost equivalent [16, 17, 18] to the BFKL and DGLAP evolution equations. The LDC approach [19, 20, 21, 22], which is a reformulation of CCFM, a unified DGLAP-BFKL approach [23, 24, 25] and the approach of doubly unintegrated parton distributions [26] are not further discussed in this report.

In the collinear approach the cross section is factorized into a process dependent hard scattering matrix element convoluted with universal parton density functions. Since strong ordering in virtualities is required in the evolution, the largest virtuality is in the hard scattering and therefore the virtuality of the partons entering the hard scattering matrix element can be neglected and they can be treated as being collinear with the incoming hadron^a. Any physics process in the fixed order collinear factorization scheme is then calculated by a convolution of a process dependent coefficient function $C^a(\frac{x}{z})$ with collinear (independent of k_t) parton density functions at a scale μ_f^2 (e.g. $\mu_f^2 = Q^2$ in $F_2(x, Q^2)$ in deep inelastic scattering (DIS)):

$$\sigma = \sigma_0 \int \frac{dz}{z} C^a(\frac{x}{z}) f_a(z, u_f^2) \quad (1)$$

While the DGLAP approach with fixed order coefficient- and splitting functions is phenomenologically successful for inclusive quantities like the structure function $F_2(x, Q^2)$ in DIS, it is not fully satisfactory from a theoretical point of view, because *“the truncation of the splitting functions at a fixed perturbative order is equivalent to assuming that the dominant dynamical mechanism leading to scaling violations is the evolution of parton cascades with strongly ordered transverse momenta”* as Catani argued in Ref. 28.

In the k_t -factorization approach, the partons along the parton ladder are no longer ordered in transverse momentum. At large energies (small x) the evolution of parton densities proceeds over a large region in rapidity $\Delta y \sim \log(1/x)$ and effects of finite transverse momenta of the partons may become increasingly important. Cross sections can then be k_t - factorized [10, 11, 8, 9] into an off mass-shell (k_t dependent) partonic cross section $\hat{\sigma}(\frac{x}{z}, k_t)$ and a k_t - unintegrated parton density function $\mathcal{F}(z, k_t)$:

$$\sigma = \int \frac{dz}{z} d^2 k_t \hat{\sigma}(\frac{x}{z}, k_t) \mathcal{F}(z, k_t) \quad (2)$$

The unintegrated gluon density $\mathcal{F}(z, k_t)$ is described by the BFKL evolution equation in the region of asymptotically large energies (small x).

An appropriate description valid for both, small and large x , is given by the CCFM evolution equation, resulting in an unintegrated gluon density $\mathcal{A}(x, k_t, \bar{q})$,

^aHowever neglecting the transverse momentum of the partons even in the collinear approach has been criticized in Ref. 27 as being unnecessary and unphysical.

which is a function also of the additional evolution scale \bar{q} described below. This scale \bar{q} is connected to the factorization scale μ_f in the collinear approach.

Carrying out the k_t integration in eq.(2) explicitly, a form fully consistent with collinear factorization can be obtained [28, 29]: the coefficient functions and also the DGLAP splitting functions leading to $f_a(z, \mu_f^2)$ are no longer evaluated in fixed order perturbation theory but supplemented with the all-order resummation of the $\alpha_s \log 1/x$ contribution at small x .

2. The CCFM evolution equation

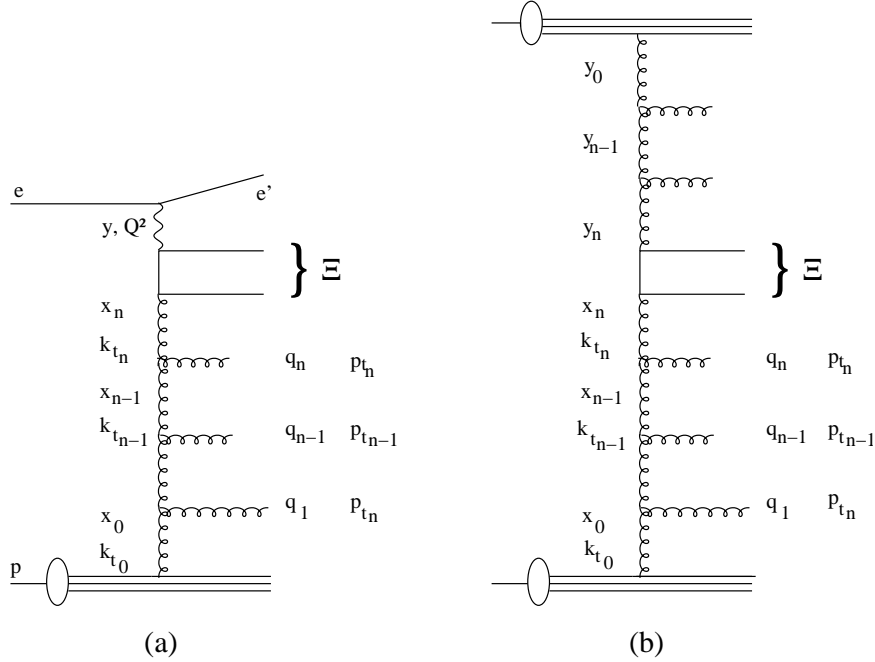


Fig. 1. Kinematic variables for multi-gluon emission in lepton production (a.) and hadron production (b). The t -channel gluon four-vectors are given by k_i and the gluons emitted in the initial state cascade have four-vectors p_i . The maximum angle (a function of the rapidity) for any emission is obtained from the quark box, as indicated with Ξ .

The pattern of QCD initial-state radiation in a small- x event in ep and $p\bar{p}$ collisions is illustrated in Fig. 1 together with labels for the kinematics. According to the CCFM evolution equation, the emission of partons during the initial cascade is only allowed in an angular-ordered region of phase space. In terms of Sudakov variables the quark pair momentum is written as:

$$p_q + p_{\bar{q}} = \Upsilon(p^{(1)} + \Xi p^{(2)}) + Q_t \quad (3)$$

4 Hannes Jung

where $p^{(1)}$ and $p^{(2)}$ are the four-vectors of incoming particles (electron-proton or proton-proton), respectively and Q_t is the transverse momentum of the quark pair in the center of mass frame of $p^{(1)}$ and $p^{(2)}$ (cms). The variable Ξ is related to the rapidity Y in the cms via

$$Y = \frac{1}{2} \log \left(\frac{E + P_z}{E - P_z} \right) = \frac{1}{2} \log \left(\frac{1}{\Xi} \right) \quad (4)$$

since $E + p_z = 2\Upsilon\sqrt{s}$, $E - p_z = 2\Upsilon\Xi\sqrt{s}$ and $E = \sqrt{s}/2$ with $s = (p^{(1)} + p^{(2)})^2$ being the squared center of mass energy. Therefore Ξ can be used to define the maximum allowed angle in the evolution. The momenta p_i of the gluons emitted during the initial state cascade are given by (here treated massless):

$$p_i = v_i(p^{(1)} + \xi_i p^{(2)}) + p_{ti}, \quad \xi_i = \frac{p_{ti}^2}{s v_i^2}, \quad (5)$$

with $v_i = (1 - z_i)x_{i-1}$ and $x_i = z_i x_{i-1}$. The variables x_i and v_i are the momentum fractions of the exchanged and emitted gluons, while z_i is the momentum fraction in the branching $(i-1) \rightarrow i$ and p_{ti} is the transverse momentum of the emitted gluon i . Again the rapidities y_i are given by $y_i = -0.5 \log \xi_i$ in the cms.

The angular-ordered region is then specified by (Fig. 1a and the lower part of the cascade in Fig. 1b, for the upper part the variables have to be changed accordingly):

$$\xi_0 < \xi_1 < \dots < \xi_n < \Xi \quad (6)$$

which becomes:

$$z_{i-1} q_{i-1} < q_i \quad (7)$$

where the rescaled transverse momentum q_i of the emitted gluon is defined by:

$$q_i = x_{i-1} \sqrt{s \xi_i} = \frac{p_{ti}}{1 - z_i} \quad (8)$$

The CCFM equation for the unintegrated gluon density can be written [15, 30, 31, 24] as an integral equation:

$$\mathcal{A}(x, k_t, \bar{q}) = \mathcal{A}_0(x, k_t, \bar{q}) + \int \frac{dz}{z} \int \frac{d^2 q}{\pi q^2} \Theta(\bar{q} - zq) \Delta_s(\bar{q}, zq) \tilde{P}_{gg}(z, q, k_t) \mathcal{A}\left(\frac{x}{z}, k'_t, q\right) \quad (9)$$

with $\vec{k}'_t = |\vec{k}_t + (1 - z)\vec{q}|$ and \bar{q} being the upper scale for any emission:

$$\bar{q} > z_n q_n, \quad q_n > z_{n-1} q_{n-1}, \quad \dots, \quad q_1 > Q_0 \quad (10)$$

The Sudakov form factor Δ_s is given by:

$$\Delta_s(\bar{q}, Q_0) = \exp \left(- \int_{Q_0^2}^{\bar{q}^2} \frac{dq^2}{q^2} \int_0^{1 - Q_0/q} dz \frac{\bar{\alpha}_s(q(1 - z))}{1 - z} \right) \quad (11)$$

with $\bar{\alpha}_s = \frac{3\alpha_s}{\pi}$. For inclusive quantities at leading-logarithmic order the Sudakov form factor cancels against the $1/(1 - z)$ collinear singularity of the splitting function.

The splitting function P_{gg} for branching i is given by:

$$P_{gg}(z_i, q_i, k_{ti}) = \frac{\bar{\alpha}_s(k_{ti})}{z_i} \Delta_{ns}(z_i, q_i, k_{ti}) + \frac{\bar{\alpha}_s(p_{ti})}{1 - z_i} \quad (12)$$

with $p_{ti} = q_i(1 - z_i)$ and the non-Sudakov form factor Δ_{ns} defined as:

$$\log \Delta_{ns}(z_i, q_i, k_{ti}) = -\bar{\alpha}_s \int_{z_i}^1 \frac{dz'}{z'} \int \frac{dq^2}{q^2} \Theta(k_{ti} - q) \Theta(q - z' q_i) \quad (13)$$

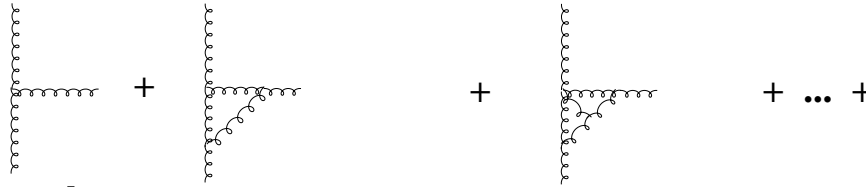
The upper limit of the z' integral is constrained by the Θ functions in eq.(13) by: $z_i \leq z' \leq \min(1, k_{ti}/q_i)$, which results in the following form of the non-Sudakov form factor [24]:

$$\log \Delta_{ns} = -\bar{\alpha}_s(k_{ti}) \log \left(\frac{z_0}{z_i} \right) \log \left(\frac{k_{ti}^2}{z_0 z_i q_i^2} \right) \quad (14)$$

where

$$z_0 = \begin{cases} 1 & \text{if } k_{ti}/q_i > 1 \\ k_{ti}/p_{ti} & \text{if } z_i < k_{ti}/q_i \leq 1 \\ z_i & \text{if } k_{ti}/q_i \leq z_i \end{cases}$$

The non-Sudakov form factor can be written as:



$$\bar{\alpha}_s \frac{1}{z} \left[1 + \bar{\alpha}_s \log \left(\frac{z_0}{z_i} \right) \log \left(\frac{k_{ti}^2}{z_0 z_i q_i^2} \right) + \left(\frac{1}{2!} \bar{\alpha}_s \log \left(\frac{z_0}{z_i} \right) \log \left(\frac{k_{ti}^2}{z_0 z_i q_i^2} \right) \right)^2 \dots \right]$$

where the similarity with the Sudakov form factor becomes obvious. Note however, that the Sudakov form factor Δ_s resums the large z contributions, whereas the non-Sudakov form factor Δ_{ns} resums the small z ones.

In the CCFM approach the scale \bar{q} (coming from the maximum angle) can be written as (see eq.(8)):

$$\bar{q}^2 = \Upsilon^2 \Xi s = \hat{s} + Q_t^2 \quad (15)$$

with $\hat{s} = (p_q + p_{\bar{q}})^2$ and the relation of \bar{q} to a particular choice of the factorization scale μ_f in the collinear approach becomes obvious.

2.1. Improvements to the CCFM splitting function

Originally, the CCFM splitting function P_{gg} , as given in eq.(12), included only the soft and collinear singular terms. In the asymptotic region of large energies this is a reasonable choice, but effects from non-leading contributions are expected at

6 Hannes Jung

presently accessible energies. For simplicity also the scale in α_s was chosen differently in the small and large z part of the splitting function (see eq.(12)). In Ref. 32 it was suggested to use $\mu_r = p_t = \bar{q}(1-z)$ everywhere and to include the non-singular terms in the splitting function. These changes are non-trivial as they need to be considered both in the Sudakov and non-Sudakov form factors.

In the following improvements to the originally proposed CCFM splitting function are discussed.

2.1.1. The soft region

In a DGLAP type evolution with the transverse momenta of the gluon propagators increasing from the proton towards the hard scattering, the non-perturbative region with $k_t < k_t^{cut}$ has an influence on the initial parton density only. In CCFM, due to angular ordering a kind of random walk in the propagator gluon k_t can be performed. Even during the evolution the non-perturbative region can be entered for $k_t < k_t^{cut}$. In the region of small k_t , α_s and the parton density are large, and collective phenomena, like gluon recombination or saturation might play a role. Thus, the fast increase of the parton density and the cross section is tamed. Much effort was put recently into a more detailed understanding of this special region of phase space (for example see Ref. [33, 34, 35, 36]). However, for the calculation of the unintegrated gluon density presented here, a simplified but practical approach is taken: $\alpha_s(\mu)$ is fixed for $\mu < Q_0$ and no emissions are allowed until $k_t > k_t^{cut}$ is reached.

2.1.2. The non-singular terms in P_{gg}

The P_{gg} splitting function used in the collinear approach contains also non-singular terms. Such non-singular terms can be included in the CCFM splitting function, but care has to be taken, which terms Δ_{ns} is acting on to ensure positivity of P_{gg} [32] :

$$P_{gg} = \bar{\alpha}_s(k_t) \left(\frac{(1-z)}{z} + \frac{z(1-z)}{2} \right) \Delta_{ns} + \bar{\alpha}_s(p_t) \left(\frac{z}{1-z} + \frac{z(1-z)}{2} \right) \quad (16)$$

As the splitting function is also part of Δ_{ns} and Δ_s , they need to be modified accordingly [32]. The non-Sudakov form factor including the full splitting function is then given by:

$$\log \Delta_{ns} = -\bar{\alpha}_s(k_t) \int_0^1 dz \left(\frac{1-z}{z} + \frac{z(1-z)}{2} \right) \int \frac{dq^2}{q^2} \Theta(k_t - q) \Theta(q - zq) \quad (17)$$

2.1.3. The scale in α_s

It was suggested in Ref. 32, to change the scale in α_s to $p_t = \bar{q}(1-z)$ also in the small z part of the splitting function P_{gg} :

$$P_{gg} = \frac{\bar{\alpha}_s(p_t)}{z} \Delta_{ns} + \frac{\bar{\alpha}_s(p_t)}{1-z} \quad (18)$$

As a consequence, the non-Sudakov form factor, changes from eq.(14) to [32,37]:

$$\log \Delta_{ns} = - \int_0^1 \frac{dz}{z} \int_{(z\bar{q})^2}^{k_t^2} \frac{dq^2}{q^2} \frac{1}{\log(q/\Lambda_{qcd})} \quad (19)$$

It is obvious, that a special treatment of the soft region is needed, because q can become very small, even $q < \Lambda_{qcd}$ at small values of z . However, in practical applications we observe only a small effect when changing the scale of the small z part from k_t to p_t .

2.2. The unintegrated gluon density

The CCFM evolution equations have been solved numerically [30] using a Monte Carlo method^b. The unintegrated gluon density at any x , k_t and scale \bar{q} is obtained by evolving a starting gluon distribution from the scale Q_0 according to CCFM to the scale \bar{q} . The normalization N of the input distribution as well as the starting scale Q_0 , which also acts as a collinear cutoff to define $z_{max} = 1 - Q_0/q$, need to be specified. These parameters were fitted such that the structure function F_2 as measured at H1 [39,40] and ZEUS [41,42] can be described after convolution with the off-shell matrix element in the region of $x < 5 \cdot 10^{-3}$ and $Q^2 > 4.5 \text{ GeV}^2$. According to the discussion in the last section, the following sets of CCFM unintegrated gluon densities are obtained:

- *JS2001* (Jung, Salam [30])
The splitting function P_{gg} of eq.(12) is used, with $Q_0 = 1.4 \text{ GeV}$. The soft region is defined by $k_t^{cut} = 0.25 \text{ GeV}$.
- *J2003 set 1* [43]
The CCFM splitting function containing only singular terms (eq.(12)) is used, with $k_t^{cut} = Q_0$ fitted to $k_t^{cut} = Q_0 = 1.33 \text{ GeV}$.
- *J2003 set 2* [43]
The CCFM splitting function (eq.(16)) containing also the non singular terms is used. The Sudakov and non-Sudakov form factors were changed accordingly. The collinear cut is fitted to $Q_0 = k_t^{cut} = 1.18 \text{ GeV}$.
- *J2003 set 3* [43]
CCFM splitting function containing only singular terms but the scale in α_s is changed from k_t to p_t for the $1/z$ term. The collinear cut is fitted to $Q_0 = k_t^{cut} = 1.35 \text{ GeV}$. The problematic region in the non-Sudakov form factor in eq.(14) is avoided by fixing $\alpha_s(\mu)$ for $\mu < 0.9 \text{ GeV}$.

A comparison of the different sets of CCFM unintegrated gluon densities is shown in Fig. 2. It is clearly seen, that the treatment of the soft region, defined by $k_t < k_t^{cut}$ influences the behavior at small x and small k_t . After convolution with the off-shell matrix elements, all sets describe the structure function $F_2(x, Q^2)$ reasonably

^bA Fortran program for the unintegrated gluon density $x\mathcal{A}(x, k_t, \bar{q})$ can be obtained from Ref.38.

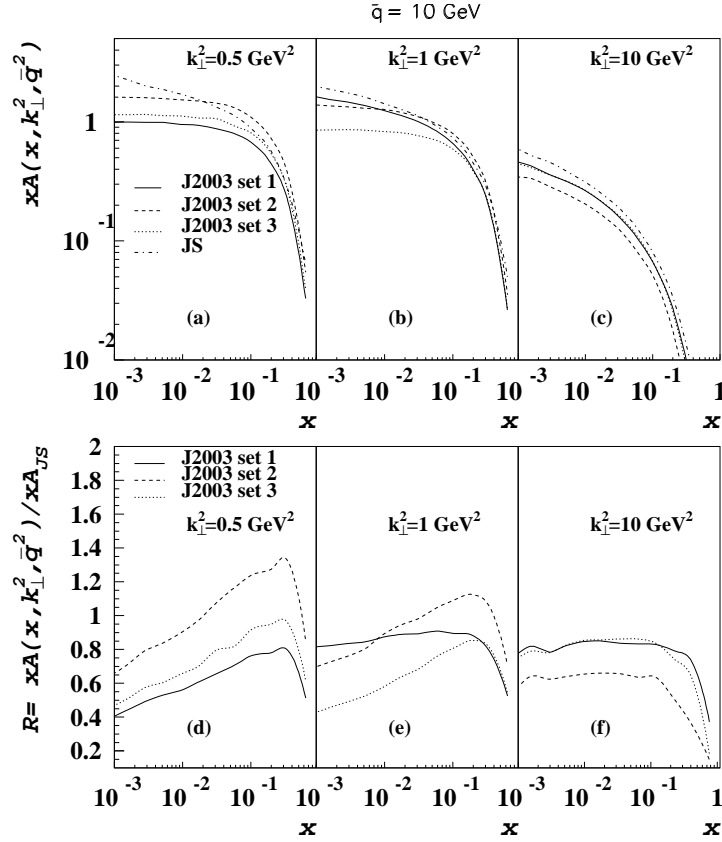


Fig. 2. Comparison of the different sets of unintegrated gluon densities obtained from the CCFM evolution as described in the text. In (a – c) the unintegrated gluon density is shown as a function of x for different values of k_t at a scale of $\bar{q} = 10$ GeV. In (d – f) the ratio $R = \frac{x\mathcal{A}(x, k_t^2, \bar{q}^2)}{x\mathcal{A}(x, k_t^2, \bar{q}^2)_{JS}}$ as a function of x for different values of k_t is shown.

well. In Fig. 3 results of the fits are compared with measurements of the structure function $F_2(x, Q^2)$ as obtained by the H1 [40] and ZEUS [42] collaborations. In Tab. 1 the parameters of the CCFM unintegrated gluon densities are summarized indicating also the quality of the fits. It is interesting to note, that the quality of the CCFM fits is similar to that obtained from global fits in the collinear DGLAP approach (e.g. Ref. 44, 45).

3. Comparison with hadronic final state data

A comparison of measurements of hadronic final state properties, like jet or heavy quark cross sections, with theoretical predictions requires a detailed simulation of the experimentally accessible phase space. Such simulations are provided by Monte Carlo event generators, which also allow to apply the hadronization step. Monte Carlo event generators for DGLAP type collinear factorized processes are widely used (e.g. PYTHIA [46], RAPGAP [47], HERWIG [48]). Two Monte Carlo generators

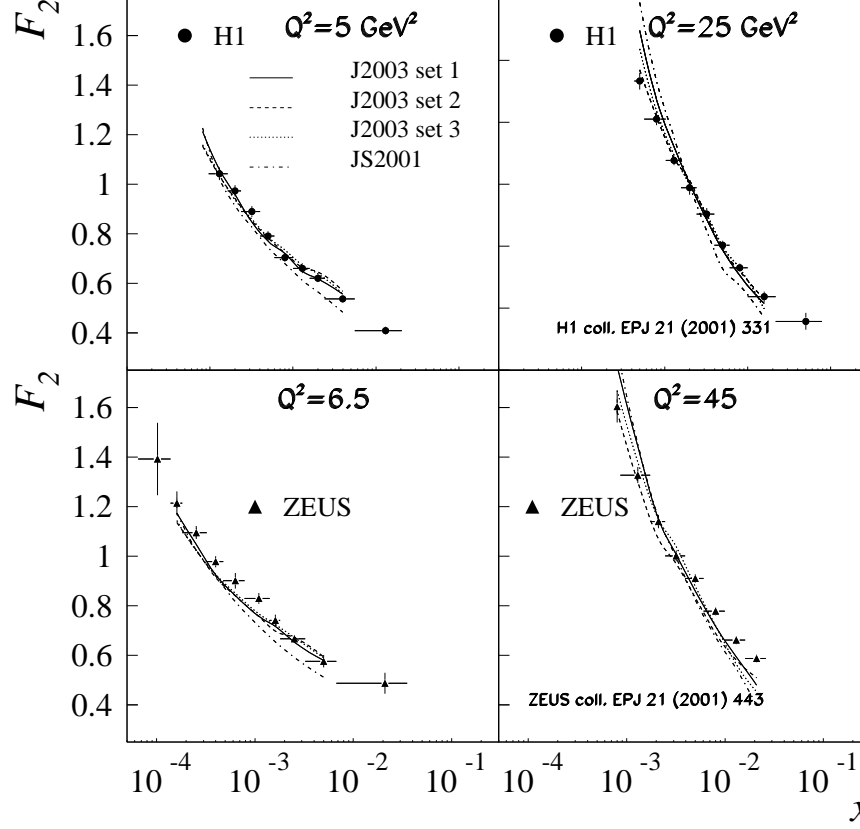


Fig. 3. The structure function $F_2(x, Q^2)$ as measured by H1 [40] and ZEUS [42] together with the results of the different fits described in Tab. 1

Table 1. Parameters of the CCFM unintegrated gluon densities. The χ^2/ndf is obtained from a comparison to HERA F_2 data [39, 40, 41, 42] in the range $x < 5 \cdot 10^{-3}$ and $Q^2 > 4.5 \text{ GeV}^2$.

set	P_{gg}	Δ_{ns}	$Q_0 \text{ (GeV)}$	$k_t^{cut} \text{ (GeV)}$	χ^2/ndf
<i>JS2001</i> [30]	eq.(12)	eq.(14)	1.40	0.25	1197/248 = 4.8
<i>J2003 set 1</i>	eq.(12)	eq.(14)	1.33	1.33	321/248 = 1.29
<i>J2003 set 2</i>	eq.(16)	eq.(17)	1.18	1.18	293/248 = 1.18
<i>J2003 set 3</i>	eq.(18)	eq.(19)	1.35	1.35	455/248 = 1.83

have been developed including the small x evolution equations: CASCADE [30, 38], which follows explicitly the CCFM approach of angular ordering and LDC [19, 20, 21, 22] which is a reformulation of CCFM (not described here). It has been shown [30], that the parton shower approach used in CASCADE reproduces exactly the properties of the CCFM evolution described in section 2. The CASCADE Monte Carlo event generator has been frequently used for comparison with HERA measurements, like

heavy quark [49, 50, 51, 52] and high p_t jet [53, 30, 54, 55] production, and also with bottom production at the Tevatron [52].

In the following sections a few examples are presented where data are compared to predictions obtained with CASCADE based on the new unintegrated gluon densities, described in section 2.2.

3.1. Jet cross section at HERA

The azimuthal correlation of dijets at HERA is sensitive to the transverse momentum of the partons incoming to the hard scattering process and therefore sensitive to the details of the unintegrated gluon density. This was studied in a measurement [54] of the cross section for dijet production with $E_T > 5(7)$ GeV in the range $1 < \eta_{lab} < 0.5$ in deep-inelastic scattering ($10^{-4} < x < 10^{-2}$, $5 < Q^2 < 100$ GeV²). In LO collinear factorization, dijets at small x_{Bj} are produced essentially by $\gamma g \rightarrow q\bar{q}$, with the gluon collinear to the incoming proton. Therefore the $q\bar{q}$ pair is produced back-to-back in the plane transverse to the γ^*p direction. From NLO ($\mathcal{O}(\alpha_s^2)$) on, significant deviations from the back-to-back scenario can be expected. In the k_t -factorization approach the transverse momentum of the incoming gluon, described by the unintegrated gluon density, is taken explicitly into account, resulting in deviations from a pure back-to-back configuration. The azimuthal decorrelation, as suggested in Ref. 56, can be measured:

$$S = \frac{\int_0^\alpha N_{2-jet}(\Delta\phi^*, x, Q^2) d\Delta\phi^*}{\int_0^{180^\circ} N_{2-jet}(\Delta\phi^*, x, Q^2) d\Delta\phi^*}, 0 < \alpha < 180^\circ \quad (20)$$

In the measurement shown in Fig. 4, $\alpha = 120^\circ$ has been chosen. The data are compared to predictions from CASCADE using *J2003 set 1 - 3*. Also shown for comparison is the NLO-dijet [57] calculation of the collinear approach. One clearly sees, that a fixed order NLO-dijet calculation is not sufficient, whereas *J2003 set 2* gives a good description of the data. However, the variable S is sensitive to the details of the unintegrated gluon distribution, as can be seen from the comparison with *J2003 set 1* and *set 3*.

A measurement, aiming to observe deviations from the collinear DGLAP approach, is the production of jets in the forward (proton) region. The phase space is restricted to a region of $Q^2 > 5$ GeV² and $E_T^{jet} > 3.5$ GeV in the forward region of $1.7 < \eta_{jet} < 2.8$ with the additional requirement of $0.5 < E_{T,jet}^2/Q^2 < 2$, a region where the contribution from the evolution in Q^2 is small. The cross section for forward jet production has been measured by H1 [53] as a function of x_{Bj} , shown in Fig. 5 together with predictions from CASCADE using *J2003 set 1 - 3*. Also the NLO-dijet [57] prediction in the collinear approach is shown. The fixed NLO-dijet calculation falls below the measurement, whereas the k_t -factorization approach supplemented with CCFM evolution gives a reasonable description of the data for all *J2003 set 1 - 3*.

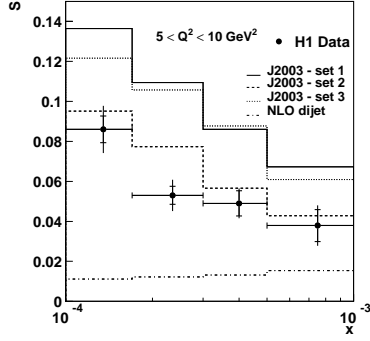


Fig. 4. The S distribution for dijet events [54]. The prediction from CASCADE using *J2003 set 1* and *J2003 set 2* are shown together with the NLO-dijet prediction in the collinear factorization approach.

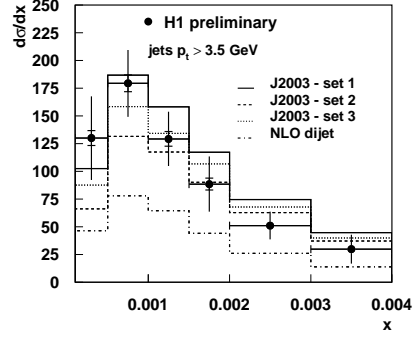


Fig. 5. The cross section for forward jet production as measured by H1 [53] as a function of x_{Bj} . The prediction are the same as in Fig. 4.

3.2. Charm Production at the Tevatron

The differential cross section as a function of the transverse momentum of D -mesons has been measured in $p\bar{p}$ collisions at $\sqrt{s} = 1.96$ TeV by the CDF collaboration [58]. They find the measured cross section to be larger than the NLO predictions in the collinear factorization approach by about 100 % at low p_t and 50 % at high p_t . In Fig. 6 the measurement is shown together with the predictions obtained in k_t -factorization using CASCADE with the CCFM unintegrated gluon density described above. For *J2003 set 1* and *set 3* good agreement for all measured charmed mesons is observed. The cross section predicted using *J2003 set 2* falls below the measurement, in contrast to the observation in Fig. 4, showing the sensitivity of the measurements on the details of the unintegrated gluon density.

3.3. Bottom Production at the Tevatron

The cross section for $b\bar{b}$ production in $p\bar{p}$ collision at $\sqrt{s} = 1800$ GeV has also been compared with the prediction of CASCADE based on the CCFM gluon densities. Since CASCADE generates full hadron level events, direct comparisons with measured cross sections for the production of b quarks decaying semi-leptonically into muons are possible. The muon cross sections as a function of the transverse momentum p_T^μ and pseudo-rapidity $|y^\mu|$ as measured by D0 [59] are compared to the CASCADE prediction in Fig. 7 and Fig. 8. Both the p_T^μ and $|y^\mu|$ cross sections are well described with *J2003 set 1* and *set 3*. The prediction based on *J2003 set 2* falls below the measurement, as was already observed in the charm case, again indicating the sensitivity to the details of the unintegrated gluon density.

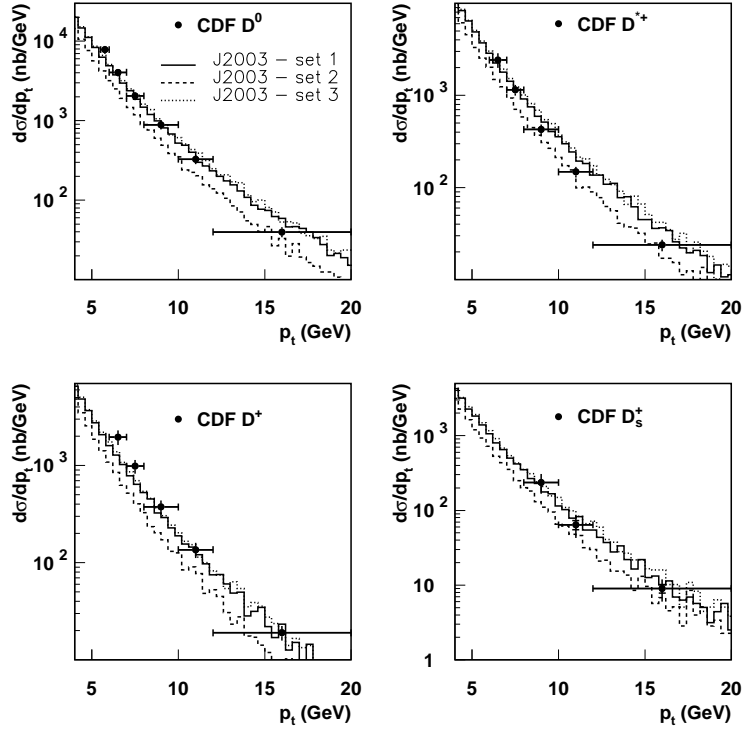


Fig. 6. Differential cross section for D meson production as measured by CDF [58] as a function of the transverse momentum compared to predictions from CASCADE.

3.4. Higgs production in $p\bar{p}$

Higgs production at high energies proceeds predominantly via gluon - gluon scattering. Much effort has been put into the calculation of higher order corrections in the collinear approach, not only for the calculation of the total production cross section, but also for the calculation of the transverse momentum spectrum of the Higgs boson [60,61,62]. At the large Tevatron or LHC energies and with an expected Higgs mass of $\mathcal{O}(100 - 200)$ GeV, the k_t -factorization approach can be also used to estimate higher order corrections. The off-mass-shell matrix element $g^*g^* \rightarrow h$ has been calculated in Ref. 63 in the high energy approximation for $m_t \rightarrow \infty$ and is now implemented in CASCADE. In Fig. 9 the distribution of the longitudinal momentum fractions x of the gluons and their transverse momenta are shown for Tevatron and LHC energies. In both cases, the longitudinal momenta reach values of the same order as the average transverse momenta ($\sim 10(18)$ GeV for Tevatron (LHC) energies, respectively), making the k_t -factorization approach applicable. It can be seen in Fig. 9, that the k_t spectrum of the gluons is different for the different unintegrated gluon densities described in sec. 2.2, both in the small and also large

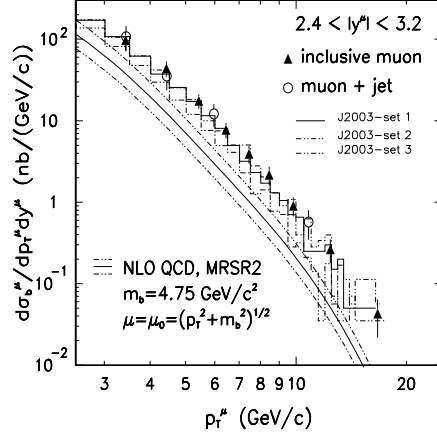


Fig. 7. Cross section for muons from b -quark decays as a function of p_T^μ (per unit rapidity) as measured by D0 [59] compared to the prediction of CASCADE.

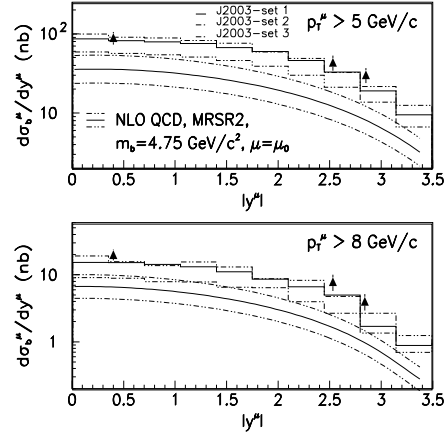


Fig. 8. Cross section for muons from b -quark decays as a function of $|y^\mu|$ for two different p_T^μ cuts as measured by D0 [59] compared to the prediction of CASCADE.

Table 2. Cross section for Higgs boson production $\sigma(pp \rightarrow hX)$

gluon distribution	\sqrt{s}	
	1.96 TeV	14.0 TeV
J2003 set 1	0.47 pb	22.6 pb
J2003 set 2	0.38 pb	7.8 pb
J2003 set 3	0.54 pb	24.6 pb

k_t region. In Fig. 10 the differential cross section for Higgs production as a function of p_t obtained with CASCADE is shown for the different unintegrated gluon densities. The total cross section for Higgs production is given in Tab. 2. It is interesting to note, that the different set of unintegrated gluon densities predict similar cross sections as a function of p_t for Tevatron energies whereas at LHC the cross section differs by factors up to 3. This again clearly indicates the sensitivity to the details of the unintegrated gluon density, which can be determined much more precisely with the forthcoming measurements at HERA. A similar result has been obtained in Ref. 64, 65, approximating the matrix element and the CCFM unintegrated gluon distribution and also applying doubly unintegrated parton distributions in Ref. 66.

4. Conclusion

It has been shown, that k_t -factorization and the CCFM evolution of the gluon density is a powerful tool for the description of hadronic final state measurements. The

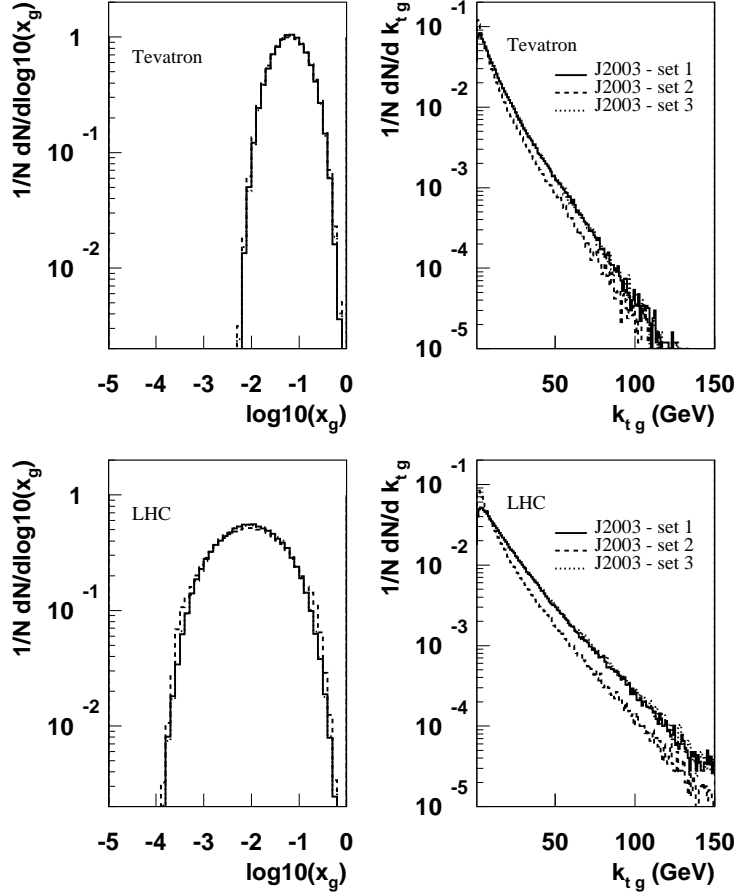


Fig. 9. Longitudinal and transverse momenta of the gluons for $g^*g^* \rightarrow h$ for Tevatron (upper) and LHC (lower) energies.

unintegrated gluon densities, which are obtained from CCFM evolution convoluted with the off-mass-shell matrix elements to describe HERA F_2 data are implemented in the full hadron level Monte Carlo event generator CASCADE.

Jet measurements at HERA, but also measurements of charm and bottom production at the Tevatron can be reasonably well described (with specific sets of unintegrated gluon densities), whereas calculations performed in the collinear approach even in NLO have difficulties to describe the data. This shows the advantage of applying k_t -factorization to estimate higher order contributions to the cross section but also the importance of a detailed understanding of the parton evolution process.

The same unintegrated gluon densities have been used to calculate also the transverse momentum spectrum of the Higgs boson production at the Tevatron and the LHC. Given the large transverse momenta of the gluons involved, k_t -factorization is

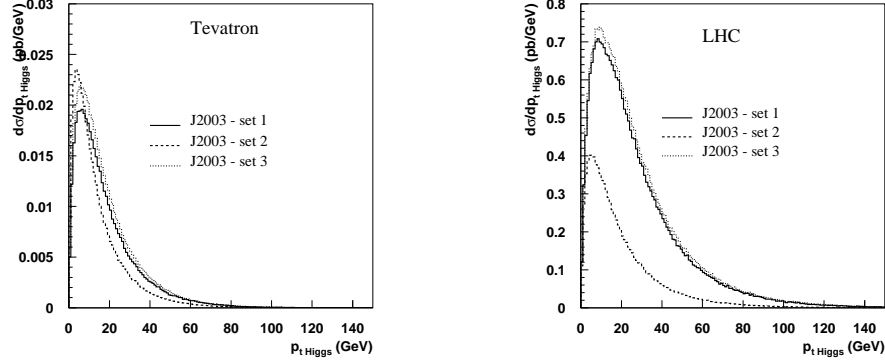


Fig. 10. Differential cross section for Higgs production as a function of the transverse momentum for $m_{Higgs} = 125$ GeV obtained with the different un-integrated gluon densities.

the appropriate tool for calculating higher order corrections. However, the different unintegrated gluon densities show significant effects at LHC energies, indicating the need for better experimental constraints as well as further theoretical studies for a more detailed understanding of parton evolution at large energies.

Acknowledgments

I wish to thank R Godbole for drawing my interest to Higgs production in the k_t -factorization approach. I am grateful to F Hautmann for explanations of his calculation of Higgs production in k_t -factorization. I wish to thank J Gayler and L Jönsson for many comments and a careful reading of the manuscript and the DESY directorate for hospitality and support..

References

1. V. Gribov, L. Lipatov, *Sov. J. Nucl. Phys.* **15** (1972) 438 and 675.
2. L. Lipatov, *Sov. J. Nucl. Phys.* **20** (1975) 94.
3. G. Altarelli, G. Parisi, *Nucl. Phys.* **B 126** (1977) 298.
4. Y. Dokshitzer, *Sov. Phys. JETP* **46** (1977) 641.
5. E. Kuraev, L. Lipatov, V. Fadin, *Sov. Phys. JETP* **44** (1976) 443.
6. E. Kuraev, L. Lipatov, V. Fadin, *Sov. Phys. JETP* **45** (1977) 199.
7. Y. Balitskii, L. Lipatov, *Sov. J. Nucl. Phys.* **28** (1978) 822.
8. S. Catani, M. Ciafaloni, F. Hautmann, *Nucl. Phys.* **B 366** (1991) 135.
9. J. Collins, R. Ellis, *Nucl. Phys.* **B 360** (1991) 3.
10. L. Gribov, E. Levin, M. Ryskin, *Phys. Rep.* **100** (1983) 1.
11. E. M. Levin, M. G. Ryskin, Y. M. Shabelski, A. G. Shuvaev, *Sov. J. Nucl. Phys.* **53** (1991) 657.
12. M. Ciafaloni, *Nucl. Phys.* **B 296** (1988) 49.
13. S. Catani, F. Fiorani, G. Marchesini, *Phys. Lett.* **B 234** (1990) 339.
14. S. Catani, F. Fiorani, G. Marchesini, *Nucl. Phys.* **B 336** (1990) 18.
15. G. Marchesini, *Nucl. Phys.* **B 445** (1995) 49.

16 Hannes Jung

16. J. R. Forshaw, A. Sabio Vera, *Phys. Lett.* **B440** (1998) 141.
17. B. R. Webber, *Phys. Lett.* **B444** (1998) 81.
18. G. Salam, *JHEP* **03** (1999) 009.
19. B. Andersson, G. Gustafson, J. Samuelsson, *Nucl. Phys.* **B 467** (1996) 443.
20. B. Andersson, G. Gustafson, H. Kharraziha, J. Samuelsson, *Z. Phys.* **C 71** (1996) 613.
21. G. Gustafson, H. Kharraziha, L. Lönnblad, The LCD Event Generator, in *Proc. of the Workshop on Future Physics at HERA*, edited by A. De Roeck, G. Ingelman, R. Klanner (1996), p. 620.
22. H. Kharraziha, L. Lönnblad, *JHEP* **03** (1998) 006.
23. J. Kwiecinski, A. Martin, A. Stasto, *Phys. Rev.* **D 56** (1997) 3991.
24. J. Kwiecinski, A. Martin, P. Sutton, *Phys. Rev.* **D 52** (1995) 1445.
25. M. A. Kimber, A. D. Martin, M. G. Ryskin, *Phys. Rev.* **D63** (2001) 114027.
26. G. Watt, A. D. Martin, M. G. Ryskin, *Eur. Phys. J.* **C31** (2003) 73.
27. J. C. Collins, X.-M. Zu, *JHEP* **06** (2002) 018.
28. S. Catani, Aspects of QCD, from the Tevatron to LHC, in *Proceedings of the International Workshop Physics at TeV Colliders* (Les Houches, France, 8-18 June, 1999), hep-ph/0005233.
29. S. Catani, k_t -factorisation and perturbative invariants at small x , in *Proceedings of the International Workshop on Deep Inelastic Scattering*, DIS 96 (Rome, Italy, 15-19 April, 1996), hep-ph/9608310.
30. H. Jung, G. Salam, *Eur. Phys. J.* **C 19** (2001) 351, hep-ph/0012143.
31. G. Bottazzi, G. Marchesini, G. Salam, M. Scorletti, *JHEP* **12** (1998) 011, hep-ph/9810546.
32. B. Andersson *et al.* [Small x Collaboration], *Eur. Phys. J.* **C 25** (2002) 77, hep-ph/0204115.
33. Y. V. Kovchegov, *Phys. Rev.* **D60** (1999) 034008.
34. I. Balitsky, *Nucl. Phys.* **B463** (1996) 99.
35. J. Andersen *et al.* [Small x Collaboration], Small x phenomenology: Summary 2002, to be published in *Eur. Phys. J. C*.
36. K. Golec-Biernat, A. M. Stasto, *Nucl. Phys.* **B668** (2003) 345.
37. H. Jung, *Acta Phys. Polon.* **B33** (2002) 2995.
38. H. Jung, *Comp. Phys. Comm.* **143** (2002) 100, <http://www.quark.lu.se/~hannes/cascade/>.
39. H1 Collaboration, S. Aid *et al.*, *Nucl. Phys.* **B 470** (1996) 3.
40. H1 Collaboration, C. Adloff *et al.*, *Eur. Phys. J.* **C 21** (2001) 33.
41. ZEUS Collaboration; M. Derrick *et al.*, *Z. Phys.* **C72** (1996) 399.
42. ZEUS Collaboration; S. Chekanov *et al.*, *Eur. Phys. J.* **C21** (2001) 443.
43. M. Hansson, H. Jung, The status of CCFM unintegrated gluon densities, DIS 2003, St. Petersburg, Russia, hep-ph/0309009.
44. A. D. Martin, R. G. Roberts, W. J. Stirling, R. S. Thorne, *Nucl. Phys. Proc. Suppl.* **79** (1999) 105, hep-ph/9906231.
45. J. Pumplin *et al.*, *JHEP* **07** (2002) 012.
46. T. Sjostrand *et al.*, *Comput. Phys. Commun.* **135** (2001) 238, hep-ph/0010017.
47. H. Jung, *The RAPGAP Monte Carlo for Deep Inelastic Scattering, version 2.08*, Lund University, 2002, <http://www.quark.lu.se/~hannes/rapgap/>.
48. G. Marchesini *et al.*, *Comp. Phys. Comm.* **76** (1992) 465, hep-ph/9912396.
49. H1 Collaboration; C. Adloff *et al.*, *Phys. Lett.* **B528** (2002) 199, hep-ex/0108039.
50. S. P. Baranov *et al.*, *Eur. Phys. J.* **C24** (2002) 425, DESY 02-017, hep-ph/0203025.
51. H. Jung, Heavy quark production at HERA in $k(t)$ factorization supplemented with

- CCFM evolution, 2001, hep-ph/0110345.
52. H. Jung, *Phys. Rev. D* **65** (2002) 034015, DESY-01-136, hep-ph/0110034.
 53. H. Jung, for H1 and ZEUS collaborations, *Nuclear Physics B - Proceedings Supplements* **117** (2002) 352.
 54. H1 Collaboration; A. Aktas et al., Inclusive dijet production at low Bjorken- x in deep inelastic scattering, 2003, hep-ex/0310019.
 55. K. Sedlak, *Acta Phys. Polon.* **B33** (2002) 3129.
 56. A. Szczurek, N. N. Nikolaev, W. Schafer, J. Speth, *Phys. Lett.* **B500** (2001) 254.
 57. S. Catani, M. H. Seymour, *Nucl. Phys.* **B485** (1997) 291.
 58. CDF Collaboration; D. Acosta et al., Measurement of prompt charm meson production cross sections in p anti- p collisions at $s^{1/2} = 1.96$ -TeV, 2003, hep-ex/0307080.
 59. D0 Collaboration; B. Abbott et al., *Phys. Rev. Lett.* **84** (2000) 5478.
 60. G. Bozzi, S. Catani, D. de Florian, M. Grazzini, *Phys. Lett.* **B564** (2003) 65.
 61. A. Kulesza, W. J. Stirling, (2003).
 62. S. Catani, D. de Florian, M. Grazzini, P. Nason, *JHEP* **07** (2003) 028.
 63. F. Hautmann, *Phys. Lett.* **B535** (2002) 159.
 64. A. Gawron, J. Kwiecinski, Resummation effects in Higgs boson transverse momentum distribution within the framework of unintegrated parton distributions, 2003, hep-ph/0309303.
 65. A. Gawron, J. Kwiecinski, W. Broniowski, *Phys. Rev.* **D68** (2003) 054001.
 66. G. Watt, Unintegrated partons to describe the $P(T)$ distribution of W and Z bosons at the Tevatron, hep-ph/0309096.